

CORONARY ARTERY STENTS MICROFABRICATED FROM PLANAR METAL FOIL: DESIGN, FABRICATION, AND MECHANICAL TESTING

Ken'ichi Takahata* and Yogesh B. Gianchandani

Electrical Engineering and Computer Science Department, University of Michigan, Ann Arbor, USA

ABSTRACT

This paper presents a new approach to the design and manufacture of coronary artery stents, which permits the use of planar batch fabrication technologies. Stent samples with different wall patterns have been fabricated from 50- μm thick stainless steel foil using micro-electro-discharge machining, and expanded to tubular shapes by using angioplasty balloons. The stents exhibit diameter variations of $\leq \pm 4\%$, almost zero radial recoil after deflation of the balloon, and longitudinal shrinkage of $< 3\%$ upon expansion. Loading tests reveal that the radial strengths match commercially available stents which have twice the wall thickness, while longitudinal compliance, at 0.02 m/N for a 4-mm long section of the stent, is $> 10\times$ higher.

I. INTRODUCTION

Stents are mechanical devices that are chronically implanted into arteries in order to physically expand and scaffold blood vessels that have been narrowed by plaque accumulation. Although they have found the greatest use in fighting coronary artery disease, stents are also used in blood vessels and ducts in other parts of the body. The vast majority of stents are made by laser machining of stainless steel tubes [1], creating mesh-like walls that allow the tube to be expanded radially with a balloon that is inflated during the medical procedure, known as balloon angioplasty. This fabrication approach offers limited throughput and prevents the use of substantial resources available for fabricating planar microstructures. Micro-electro-discharge machining (μEDM) is another option for cutting metal microstructures. This technique is capable of performing, with sub-micron tolerance and surface smoothness, 3D micromachining in any electrical conductors. It has, however, not been extensively used for stent production since traditional μEDM that uses single electrodes with single pulse timing circuits often suffers from even lower throughput than the laser machining.

As the authors have previously demonstrated, the throughput of μEDM can be vastly increased by using spatial and temporal parallelism, i.e. lithographically formed arrays of planar electrodes with simultaneous discharges generated at individual electrodes [2]. This paper reports a new fabrication approach that uses metal foils as starting materials for stents, which permits this parallelism to be exploited, thereby offering high throughput and repeatability. The favored mechanical characteristics including radial strength and longitudinal compliance in expanded stents have been experimentally and theoretically investigated, and are discussed with comparisons to commercial stents.

II. DESIGN & FABRICATION

The fabrication approach was to μEDM 50 μm -thick stainless steel foil into a structure that could be slipped over an angioplasty balloon and be reshaped into a cylinder when deployed in the manner of a conventional stent. This effort used type 304 steel which is very similar to the 316 steel commonly used for commercially available stents. The design challenge was to develop a planar pattern which would provide the critical mechanical characteristics of radial stiffness and longitudinal compliance in the expanded structure. Although several layouts were designed and experimentally tested, the best results in terms of mechanical characteristics (discussed later) are obtained with the design shown in Fig. 1. The pattern has two longitudinal side-beams, which are connected transversely by cross bands (Fig. 1c), each of which contains three identical involute loops. The involute shape is tailored to provide selected stress-relief during expansion of the stent to the deployment diameter, which is 2.65 mm in this case. To densely array the cross bands in the longitudinal direction for increasing radial strength, beams A_n , C_n , and E_n are designed to be longer than the others, B_n and D_n .

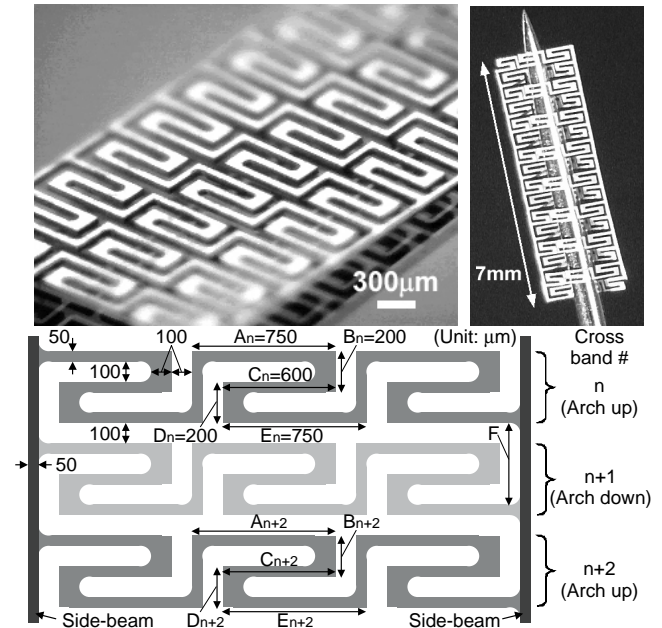


Fig. 1: Pre-expansion form of a UMich stent. (a: upper left) a fabricated sample as cut from the metal foil, (b: upper right) a needle weaved through the metal foil showing the alternating cross bands, (c: lower) a wall pattern layout and dimensions.

*Corresponding author: 1301 Beal Avenue, Ann Arbor, MI 48109-2122, USA; Tel: +1-734-647-1782; Fax: 763-9324; Email: ktakahat@eecs.umich.edu

To emulate the deployment of a stent, an angioplasty balloon is threaded through the 7mm long planar structure such that the cross bands alternate above and below it (Fig. 2a). The stent is expanded by inflating the balloon with liquid up to 12 atm. pressure, in a manner identical to commercial stents (Fig. 2b). Figure 3 shows an SEM image of the expanded stent with the balloon removed. Variation in the diameter of expanded stents was typically within $\pm 4\%$, while radial recoil upon deflation of the balloon was even smaller than that. The shrinkage in length upon the expansion was $<3\%$.

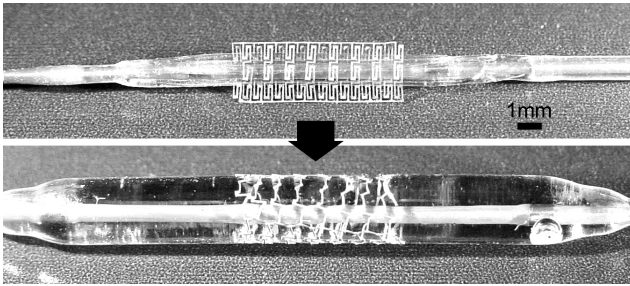


Fig. 2: Stent mounted in an angioplasty balloon. (a: upper) Before expansion, (b: lower) after expansion at 12 atm.

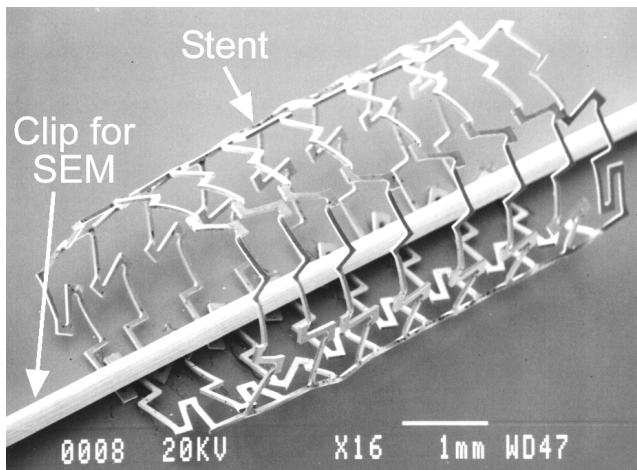


Fig. 3: Expanded state of 7-mm long stent.

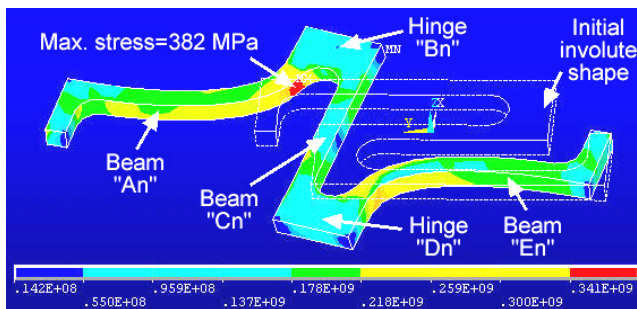


Fig. 4: FEA result of the involute beam deformation.

Upon expansion of the stent, beams in the structure are permanently deformed. The wall pattern must therefore be designed to accommodate large deformations so that the maximum *tensile* stress is less than the ultimate stress, which is about 517 MPa for the 304 stainless steel [3]. The deformation

and resultant stresses were evaluated by using an FEA package, ANSYSTM. The simulation used a bilinear stress-strain model, and the following mechanical properties of the steel [3, 4]: Young's modulus=193 GPa, yield stress=207 MPa, tangent modulus=692 MPa, and Poisson's ratio=0.27. Figure 4 shows a unit involute section with a displacement that approximately corresponds to the deployed diameter. The maximum tensile stress appears at the location indicated near the flexural hinge element B_n and is 382 MPa, sufficiently below the ultimate stress.

In addition to the bending of beam segments, torsional deformations also play important roles in expanding a stent and maintaining its final shape. The most significant ones are in the side-beams, which are twisted by 90-180° along the segment F (labeled in Fig. 1c) between two adjacent bands as shown in Fig. 5a. Figure 5b shows the torsion of another beam that was the flexural hinge of a different wall pattern. The approximate *shear* strain for both these cases is shown in Fig. 6 on a shear stress versus shear strain response curve for 304L stainless steel obtained from [5]. Although the comparison is to a macro-scale test, it is evident that beam fracture is not a concern for the stent. For the test in Fig. 5b, hinge as well as the beams had 50- μ m square cross section for the favored wall pattern. The strain due to this torsion is well below the fracture point, but since deformations at the site also include bending that may further increase the maximum strain experienced, it was appropriate to increase the safety margin. This was done by doubling the widths of the hinge elements B_n and D_n in Fig. 1c from 50 μ m to 100 μ m.

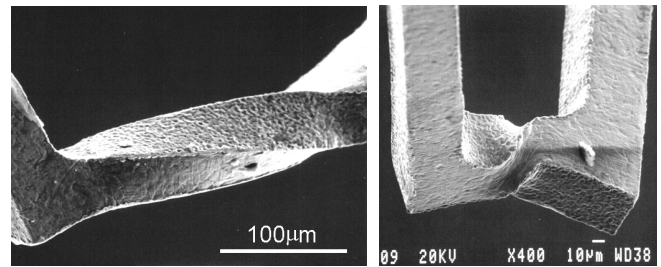


Fig. 5: Plastic deformation in torsion (a: left) segment F of a side beam in the wall pattern of Fig. 1c; (b: right) at a flexural hinge for a different wall pattern.

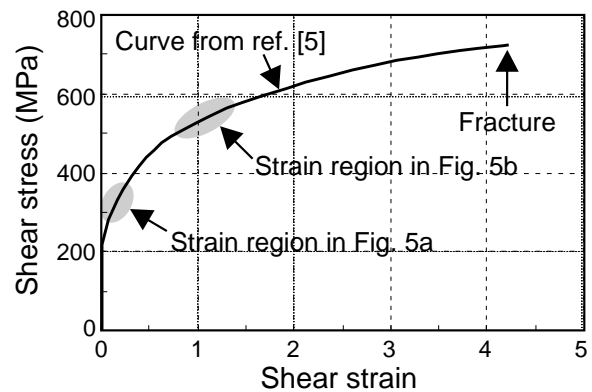


Fig. 6: Shear stress-strain curve for 304L stainless steel and approximate strain regions seen in Fig. 5.

III. EXPERIMENTAL RESULTS

The radial strength is a paramount mechanical characteristic in the stents. Several past efforts have assessed the strength in commercial stents [6, 7]. To evaluate our devices, short samples with different patterns were prepared and subjected to loading tests, in which the reaction force per unit length of the stent is measured as a function of radial deformation. A sample is held in a groove mounted on the stage and compressed toward the probe. The gauge is rigidly fixed, and the displacement of the gauge probe is negligible compared to that of the sample. The force was measured by a gauge (Imada, Inc., DPS-1) that provides 1-mN resolution while first compressing the stent by 1.5 mm in 25- μm increments, and then while relaxing the deformation.

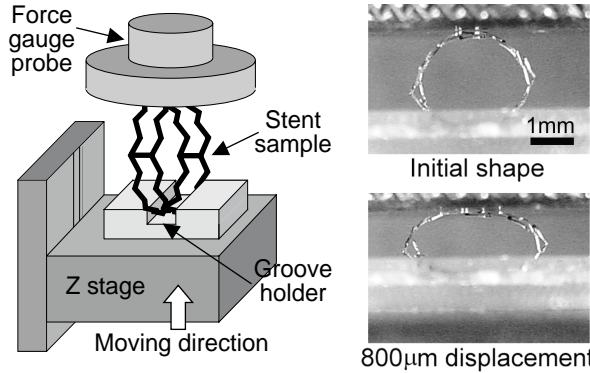


Fig. 7: (a: left) Loading test set-up, and (b: right) sample deformation in the test.

Figure 8 shows radial strength test results obtained from the stent design similar to Fig. 1, which uses 50 μm thick 304 stainless steel. A commercial stent with 316 stainless steel of thickness varying over 90-130 μm was tested for comparison. Measurements demonstrate that the UMich stent has the same radial strength even though its walls are only 50 μm thick. In addition, the UMich stent exhibits better elastic recovery after loading, which suggests that it has better radial elasticity but the same stiffness as the commercial one.

Orientation dependence of the radial strength was a concern for the UMich stent since it was shaped from a planar sheet. Identical samples were tested at two different orientations as shown in Fig. 9: (A) perpendicular to a plane that includes both side-beams, and (B) parallel to the plane. The measurements demonstrate that the radial strength is similar in both cases.

The experimental results in Fig. 8 show a few large steps in the response curve. As can be seen in Fig. 4, beams that correspond to C_n in Fig. 1c are designed to rotate about their center by $\sim 90^\circ$ after the expansion. As a result, hinges D_n and B_{n+2} are positioned closely to each other. In addition, alternate cross bands in Fig. 1c, which adjoin each other when they are mounted on the balloon, deform in a way that the gaps between their segments are reduced as the stent expands. (In fact, the side beams assume wave-like shapes as this happens.) The combination of these effects results in increased probability of physical contact between the hinges D_n and B_{n+2} . As loading is

applied, hinges happen to come into contact and get intermeshed, and then snap apart as the loading is further increased. This particular sample had reduced gaps of 50 μm between the cross bands, which could also contribute to increase the probability. This undesirable mechanical interaction however can be improved by optimizing the layout.

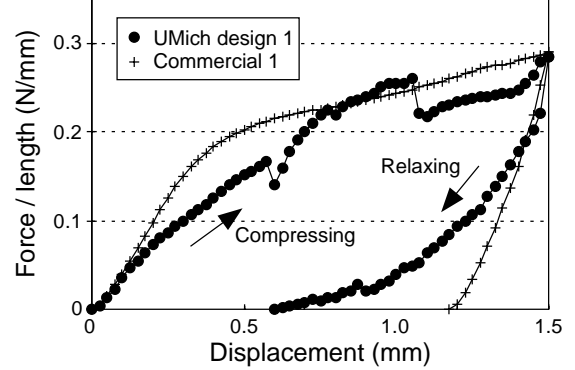


Fig. 8: Comparison of radial strength between the developed stent and a commercial stent with similar diameter.

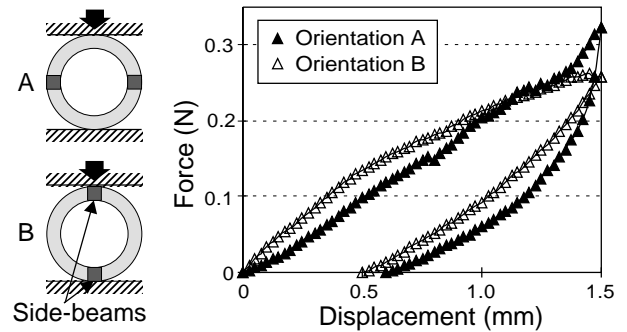


Fig. 9: Radial strength in two different orientations.

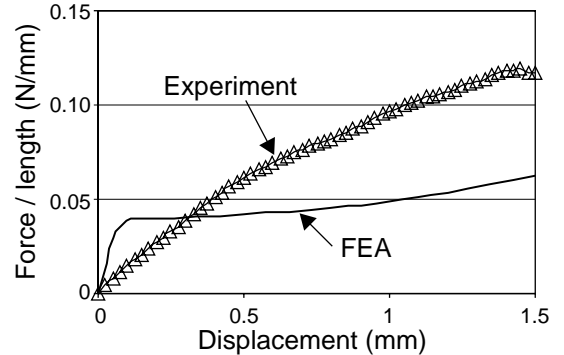


Fig. 10: FEA result using a continuum model of the wall.

To evaluate the experimental results, a loading test was simulated using ANSYSTM. In this effort a simple cylindrical shell with the same diameter, wall thickness and steel volume as the sample evaluated in Fig. 9, but with unpatterned walls, was used for simplifying the analysis. In the simulation, the cylindrical shell was radially compressed between two parallel rigid planes. Comparing the simulation to the experiment (Fig. 10), it is observed that the former exhibits a distinct yield point

at a displacement of 0.1 mm, whereas the latter curve shows no distinct yield point. This difference may be due to the pre-loading process in the real sample, i.e. the original expansion for deployment: the Bauschinger effect [8] dictates that once a tensile load is applied to a steel structure to the point of plastic deformation, in the subsequent application of a compressive load, the change in slope of the stress-strain response curve that is associated with the yield point will occur at lower values and will be less distinct.

Longitudinal compliance is a favored characteristic in stents. This is because the stent, fitted on an angioplasty balloon in a state that is only slightly expanded, must often travel a convoluted path along a blood vessel in order to reach the location of the deployment. In addition, longitudinal flexibility in a fully expanded stent can be beneficial for its deployment at curved sites. The longitudinal compliance of the fabricated stents was tested using the set-up shown in Fig. 11. A fully-expanded 7-mm long stent of the type shown in Fig. 3 was attached to a holder such that a 4-mm segment out of it was overhanging and unsupported. Using the same force gauge as in Fig. 7, the displacement response was plotted for an end load as shown in Fig. 11. A similar test was also applied to the commercial stent tested before. The results reveal that the UMich stent had spring constants of 50 N/m and <5 N/m depending on the orientation (Fig. 9), whereas that in the commercial stent resulted in 515 N/m. While this test was only performed on expanded stents, it suggests that the UMich stent will perform favorably in this respect.

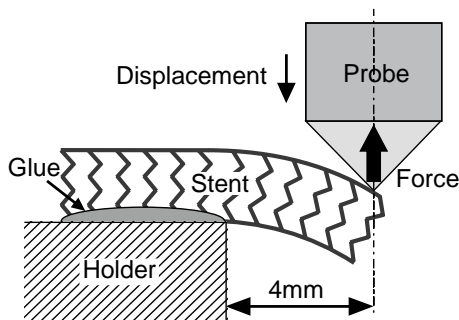


Fig. 11: Set-up for longitudinal compliance test.

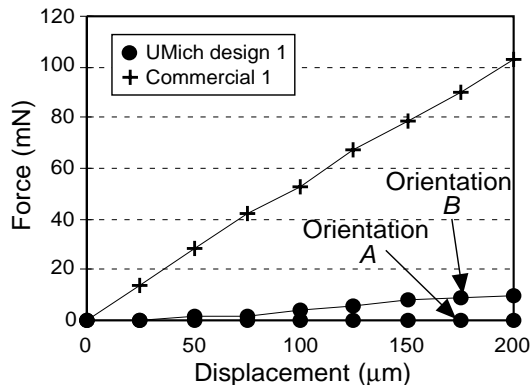


Fig. 12: Comparison of the longitudinal compliance.

IV. CONCLUSION

The design and fabrication of coronary artery stents based on use of planar stainless steel foil and μ EDM technology has been investigated. The devices are intended to be compatible with standard stenting tools and procedures. The wall patterns were designed using FEA so that both the stress relief and the mechanical strength are simultaneously achieved in the expansion. Devices consist of involute bands tied between a pair of side-beams. Measurements demonstrate that the best UMich designs have the same radial strength as a commercial stent even though the former use metal that is only about half as thick. The thinner walls also contributed to achieving at least 10X higher longitudinal flexibility than a commercial one in the expanded state. Both the radial strength and the flexibility are found to have no significant dependence on orientation relative to the original planar direction of the foil. Dimensional variations in tubular diameter, longitudinal shrinkage, and radial recoiling in the expanded stents are at most a few percent.

All devices tested in this effort were fabricated by μ EDM, which can open a path to exploit photolithography-based fabrication resources for the stent production [2]. The extension of this technology to manufacture stents will also facilitate other 3D structures such as antennas and transformers.

ACKNOWLEDGEMENTS

The authors thank Dr. Mauro Moscucci of the Cardiovascular Center at the University of Michigan Health System for his advice and discussion of stents, and also thank Mr. Vivek Sankaran for his work on preparation of samples and the test set-up.

REFERENCES

- [1] Y.P. Kathuria, "Laser Microprocessing of Stent for Medical Therapy", Proc. IEEE Int'l Symp. Micromech. Human Sci., 1998, pp. 111-114
- [2] K. Takahata, Y.B. Gianchandani, "Batch Mode Micro-Electro-Discharge Machining" J. Microelectromechanical Systems, Vol. 11, No. 2, 2002, pp.102-110
- [3] R.C. Hibberler, "Mechanics of Materials Third Edition" Prentice-Hall, Inc., 1997
- [4] S.N. David Chua, B.J. Mac Donald, M.S.J. Hashmi, "Finite-element simulation of stent expansion" J. Materials Processing Tech., Vol. 120, 2002, pp. 335-340
- [5] "Metals Handbook Ninth Edition" Vol. 8 Mechanical Testing, American Society for Metals, 1985, pp. 162
- [6] F. Flueckiger, H. Sternthal, G.E. Klein, M. Aschauer, D. Szolar, G. Kleinhapfl, "Strength, Elasticity, and Plasticity of Expandable Metal Stents: In Vitro Studies with Three Types of Stress", J. Vasc. Intervent. Radiol., Vol. 5, No. 5, 1994, pp. 745-750
- [7] R. Rieu, P. Barragan, C. Masson, J. Fuseri, V. Garitey, M. Silvestri, P. Roquebert, J. Sainsous, "Radial Force of Coronary Stents: A Comparative Analysis" Cathet. Cardiovasc. Intervent., Vol. 46, 1999, pp. 380-391
- [8] For example: J.D. Lubahn, R.P. Felgar, "Plasticity and Creep of Metals", John Wiley & Sons, 1961, pp. 482-484